EFFICIENT IMPLEMENTATION OF DOWNLINK CDMA EQUALIZATION USING FREQUENCY DOMAIN APPROXIMATION

F. S. Al-kamali[+], M. I. Dessouky, B. M. Sallam, and F. E. El-Samie[++]
Department of Electrical Communications
Faculty of Electronic Engineering
Menoufia University
Menouf, Egypt
E-mails: [+]faisalalkamali@yahoo.com, [++]fathi_sayed@yahoo.com

ABSTRACT

A signal transimitted through a wireless channel may be severely distorted due to intersymbol interference (ISI) and multiple access interference (MAI). In this paper, we propose an efficient CDMA receiver based on a frequency domain equalization with a regularized zero forcing equalizer and unit clipper decision with parallel interference cancellation (FDE-RZF-CPIC) to combat both ISI and MAI. This receiver is suitable for downlink zero padding CDMA (ZP-CDMA) cellular systems. The effects of the decision function, the channel estimation, the number of cancelled users, and the user loading on the performance of the proposed receiver are discussed in the paper. The bit error rate (BER) performance of the proposed receiver is evaluated by computer simulations. It has been found that the proposed receiver provides a good BER performance, even at a large number of interfering users. At a BER of 10^{-3}, the performance gain of the proposed receiver is about 2 dB over the RAKE receiver with clipper decision and parallel interference cancellation in the half loaded case (8 users) and is much larger in the full loaded case (16 users).

Keywords: Downlink CDMA, Decision Functions, PIC, FDE-RZF, Zero Padding, Channel Estimation.

1 INTRODUCTION

Recently, single-carrier transmission with frequency domain equalization (FDE) has attracted much attention for its excellent performance even in strong frequency selective channels. In practice, the number of fingers in the RAKE receiver is limited because of hardware complexity. The use of an FDE can alleviate the complexity problem of the RAKE receiver arising from too many paths in a severe frequency-selective channel. It has been shown that the FDE can take the place of the conventional RAKE receiver with much improved BER performance for DS/CDMA signal reception over a severe frequency-selective channel [1-5]. This gives the CDMA with FDE the power to compete with multi carrier CDMA (MC-CDMA) in fourth generation systems. The performance of CDMA is mainly limited by the interference from other users, which is called the MAI. Therefore, PIC has to be applied in CDMA receivers [6-13].

PIC has gained a considerable attention for its potential ability to increase system capacity and its simplicity. However, the conventional PIC often suffers from the error propagation phenomena that contributes to progressively enhanced interference [12]. There are several algorithms for interference cancellation in CDMA systems [6-13]. Most of these algorithms are designed for the uplink. For uplink interference cancellation, it is assumed that the base station knows all the spreading codes of the active users. For downlink CDMA, the receiver knows only the spreading code of the desired user. As a result, PIC has been assumed to be applicable at the base station, and not at the mobile terminal where only the information stream is to be decoded and the spreading codes of the interfering users are unknown. However, in last years, many algorithms have been proposed for the estimation of the codes of the interfering users and PIC has been applied for downlink CDMA [7]. The main target of this paper is to analyze the performance of PIC for downlink CDMA with different decision functions and hence to develop an efficient receiver based on FDE and PIC that is suitable for downlink CDMA.

The remainder of this paper is organized as follows: in section 2, the system model of downlink CDMA is presented. In Section 3, the concept of PIC

is discussed. Section 4 deals with the different possible decision functions. FDE for downlink ZP-CDMA is presented in section 5. In Section 6, the proposed FDE-RZF-CPIC algorithm is presented. Channel estimation is discussed in section 7. The relative performance of the proposed receiver is compared to some existing approaches in section 8. Finally, Section 9, gives the concluding remarks.

Notations: The symbols $(.)^H$, $(.)^T$, and $(.)^{-1}$ designate complex conjugate transposition of a matrix, transposition of a matrix, and inverse of a matrix, respectively. Vectors and matrices are represented in boldface.

2 SYSTEM MODEL

In downlink CDMA, the channel is common with frequency selective fading. We assume that the channel parameters vary slowly with time, so that for sufficiently short intervals the channel is approximately a linear time-invariant system. The baseband channel response can then be expressed by Dirac delta functions as follows [9]:

$$h(t) = \sum_{w}^{W} h_w \delta(t - \tau_w) \tag{1}$$

where h_w , *and* τ_w are the complex fading and propagation delay of the *w-th* path, and W is the number of multipath components of the channel impulse response. In this paper, we assume block fading, where the path gains stay constant over one block duration. The received signal at the mobile can be written as[9]:

$$r(t) = \sum_{l}^{L} \sum_{k}^{K} \sum_{w}^{W} h_w A_k b_k(l) c(t - \tau_w) s_k(t - lT_S - \tau_w) + n(t) \tag{2}$$

where A_k is the amplitude, $b_k(l) \in \{-1,1\}$ is the lth bit, s_k (t) is the spreading code of user k, and *c(t)* is the scrambling code. In matrix form, the received signal in Eq. (2) can be written as follows [6]:

$$\mathbf{r} = \mathbf{H}_0 . \mathbf{d}_m + \mathbf{H}_1 . \mathbf{d}_{m-1} + \mathbf{n}_m \tag{3}$$

Where $\mathbf{d}_m$ is the *mth* block of the transmitted signal, $\mathbf{r}$ is the received vector, while $\mathbf{n}_m$ is the additive noise with zero mean and variance of σ^2. $\mathbf{H}$ is the (N×L)×(N×L) matrix describing a multipath channel having impulse response h(t) of length W. L is the number of symbols for each user. $N=T_S/T_c$ is the number of chips per bit (spreading factor). T_S is the symbol period. T_c is the chip period. K is the number of active users.

We can observe that inter-block interference (IBI) would disappear from Eq. (3) if the last W-1 elements of vectors $\mathbf{d}_m$ and $\mathbf{d}_{m-1}$ were equal, i.e., if a zero padding (or cyclic prefix) process is used. The length of the zero padding must be greater than W. In this paper we will use a zero padding method as in [1]. So, Eq.(3) can then be written as:

$$\mathbf{r} = \mathbf{H}\mathbf{d} + \mathbf{n} \tag{4}$$

Where $\mathbf{H}=\mathbf{H}_0+\mathbf{H}_1$ has now a circulant structure. $\mathbf{H}$ can be written as:

$$\mathbf{H} = \begin{bmatrix} h[0] & 0 & . & 0 & h[W-1] & . & . & h[0] \\ . & h[0] & . & & . & . & & . \\ . & & . & & . & & . & h[W-1] \\ h[W-1] & & & & . & . & & 0 \\ 0 & . & & & & & & . \\ . & . & . & & & & . & 0 \\ 0 & . & 0 & h[W-1] & . & . & & h[0] \end{bmatrix} \tag{5}$$

The vector $\mathbf{d}$ can be represented as:

$$\mathbf{d} = \mathbf{CSb} \tag{6}$$

Where $\mathbf{C}$ is an (N×L)×(N×L) scrambling code matrix. $\mathbf{S}$ is an (N×L)×(K×L) orthogonal code matrix, and $\mathbf{H}_1\mathbf{d}_{m-1}$ is the inter block interference (IBI) term [6]. $\mathbf{H}_0$ and $\mathbf{H}_1$ can be written as [6]:

$$\mathbf{H}_0 = \begin{bmatrix} h[0] & 0 & . & . & . & . & 0 \\ . & h[0] & & & & & \\ . & & . & & & & \\ h[W-1] & & & . & & & \\ . & . & & & . & & \\ 0 & . & . & h[W-1] & . & . & h[0] \end{bmatrix}$$

, and

$$\mathbf{H}_1 = \begin{bmatrix} 0 & . & 0 & h[W-1] & . & . & h[0] \\ . & . & & & . & & . \\ . & . & & & & . & . \\ . & & . & & & & h[W-1] \\ . & & & . & & & 0 \\ . & & & & . & & . \\ 0 & . & . & . & . & . & 0 \end{bmatrix} \tag{7}$$

The structures of the individual components in Eq. (6) are given bellow [14]:

$$\mathbf{S} = diag[\overline{\mathbf{S}}\overline{\mathbf{S}}.....\overline{\mathbf{S}}] \tag{8}$$

$$\overline{\mathbf{S}} = [\mathbf{s}_1 \mathbf{s}_2 ..... \mathbf{s}_K] \quad (9)$$

$$\mathbf{S}_k = [\mathbf{s}_k(0), \mathbf{s}_k(1), ..., \mathbf{s}_k(N-1)]^T \quad (10)$$

$$\mathbf{b} = [\mathbf{b}^T(1)\mathbf{b}^T(2).....\mathbf{b}^T(L)] \quad (11)$$

$$\mathbf{C} = diag[c(1), c(2), ..., c(N \times L)] \quad (12)$$

$$\mathbf{b}(l) = [b_1(l), b_2(l), ..., b_K(l)]^T \quad (13)$$

Where $\mathbf{S}_K$ is the signature sequence (code), and **b** is a vector consisting of the users amplitudes and the transmitted bits, and $b_K(l)$ is the *lth* bit.

In this paper, we suppose a perfect estimation of the downlink interfering codes. So, we can write the received signal as follows:

$$\mathbf{r} = \mathbf{HCS_d b_d} + \mathbf{HCU b_{int}} + \mathbf{n} \quad (14)$$

Where $\mathbf{S_d}$ is an ((N×L)×L) matrix consisting of the spreading code of the desired user, **U** is an (N×L)×((K-1)×L) matrix consisting of the spreading codes of the interfering users, $\mathbf{b_d}$ is an L×1 vector consisting of the desired symbols, and $\mathbf{b_{int}}$ is a ((K-1)×L)×1 vector consisting of the interfering symbols.

In the zero padding method, N_{ZP} zeros will be added to the end of N_F-N_{ZP} symbols to build a block of N_F symbols before transmission. At the receiver, the FFT detection will be performed on the padded data block, the detected zeros at the end of this data block will then be discarded after despreading. The zero padding process is illustrated in Fig. (1).

3 PIC FOR DOWNLINK ZP-CDMA

Parallel interference cancellation for CDMA systems has attracted much interest, due to its structured architecture that facilitates easy implementation. It was first introduced in 1990 [15]. Such multistage PIC methods attempt to cancel MAI based on tentative decisions. The idea of PIC is to estimate the multiple access and multipath induced interferences and then to subtract the interference estimate. The circulant matrix **H** can be efficiently diagonalized by the fast Fourier transform (IFFT) and inverse fast Fourier transform (FFT). Let Ψ^{-1} and Ψ denote the FFT matrix and the IFFT matrix, respectively.

A circulant matrix A can be written as (see appendix 1) :

$$\mathbf{A} = \mathbf{\Psi \Lambda \Psi}^{-1} \quad (15)$$

where Λ is the FFT of the circulant sequence of **A**.

The implementation of the RAKE receiver with PIC in frequency domain can be summarized as follows [6]:

1- Apply the RAKE receiver on the received signal as follows [14]:

$$\mathbf{d}_{RAKE} = \mathbf{\Psi}(\mathbf{\Lambda}^H \mathbf{R}_T) \quad (16)$$

Where Λ is a diagonal matrix containing the FFT of the circulant sequence of **H,** and $\mathbf{R_T}$ is the FFT of **r**.

2-Estimate all interferences as follows:

$$\hat{\mathbf{b}}_{int} = \mathbf{U}^T \mathbf{C}^H \mathbf{d}_{RAKE} \quad (17)$$

3- Discard the detected zero symbols at the end of each block to produce $\overset{L}{\mathbf{b}}_{int}$, then take the decision as follows:

$$\tilde{\mathbf{b}}_{int} = f_{dec}\{\overset{L}{\mathbf{b}}_{int}\} \quad (18)$$

where $f_{dec}(.)$ is the tentative decision function.

4- Add zeros for padding , then regenerate the MAI as follows:

$$\mathbf{r}_{MAI} = \mathbf{H}\ \mathbf{CU}\ \tilde{\mathbf{b}}'_{int} \quad (19)$$

where $\tilde{\mathbf{b}}'_{int}$ is the zero padded version of $\tilde{\mathbf{b}}_{int}$.

5- Use PIC to cancel the effects of interference on the received signal to obtain an interference free signal:

$$\mathbf{z} = \mathbf{r} - \mathbf{r_{MAI}} \quad (20)$$

6- Apply the RAKE receiver on the vector **z** as follows:

$$\mathbf{d_{RAKE}} = \mathbf{\Psi}\ (\mathbf{\Lambda}^H \mathbf{\Psi}^{-1} \mathbf{z}) \quad (21)$$

7- Descramble and despread the obtained data.

8- Finally, discard the detected zero symbols and perform hard decision.

Due to error propagation, PIC with hard decision may perform worse than PIC with linear or soft decision functions. On the other hand, hard-decision interference cancellation can completely cancel interference when the hard decisions made are correct [12].

4 DECISION FUNCTIONS

The performance of PIC depends on the decision function used in the interference cancellation iterations, e.g., hard, soft, null zone, unit clipper, and hybrid decision functions [12].

The general model for the decision function is:

$$y = f_{dec}(x) \quad (22)$$

The following, decision functions can be used:

- **The hard limiter** [12]:

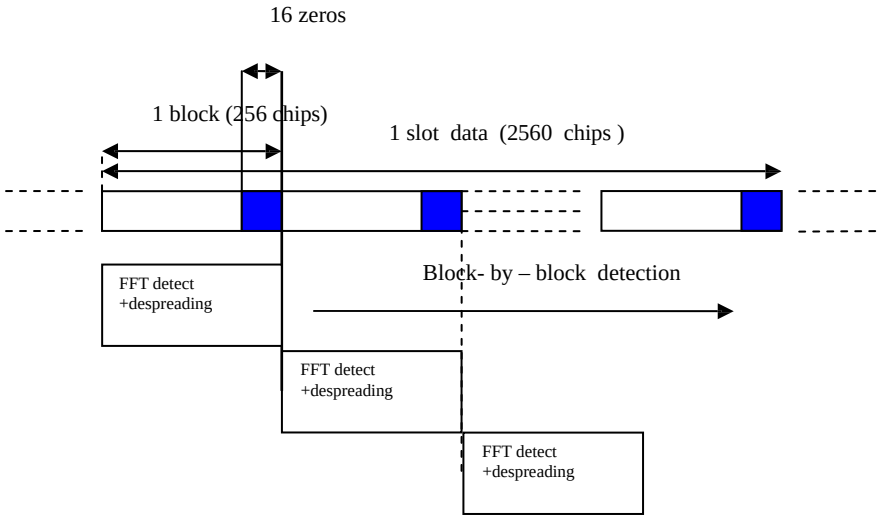

Figure 1: CDMA transmission for FDE detector using zero padding

$$y = f_{dec}(x) = \begin{cases} 1 & x \geq 0 \\ -1 & x < 0 \end{cases} \quad (23)$$

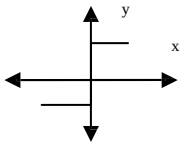

Hard Limiter

It makes a hard decision for one of the two possible symbols.

- **The null zone function** [11]:

$$y = f_{dec}(x) = \begin{cases} 1, & x > c_n \\ 0, & x \in [-c_n, c_n] \\ -1, & x < -c_n \end{cases} \quad (24)$$

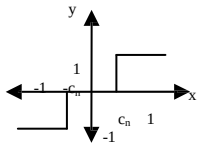

Null Zone

It makes a hard decision when the soft bit estimate lies outside the interval $[-c_n, c_n]$, and sets the decision result to zero when the soft bit estimate lies inside the interval $[-c_n, c_n]$. Where c_n is the null zone decision threshold ($0 \leq c_n \leq 1$) [11].

- **The linear decision function:**

$$y = f_{dec}(x) = x \quad (25)$$

It offers analytical access to the PIC performance, but performs worse than other decision functions.

- **The unit clipper decision function** [11]:

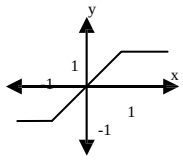

Unit Clipper

$$y = f_{dec}(x) = \begin{cases} 1, & x > 1 \\ x, & x \in [-1, 1] \\ -1, & x < -1 \end{cases} \quad (26)$$

It makes a soft bit decision when the soft bit estimate lies inside the interval [-1 , 1] to avoid propagation error , and makes a hard decision when the soft bit estimate lies outside the interval [-1 , 1] to avoid the noise magnification [10].

5 FREQUENCY DOMAIN EQUALIZER FOR DOWNLINK ZP-CDMA.

The application of FDE techniques makes single carrier modulation a potentially valuable alternative to OFDM, especially in regard to its robustness to RF implementation impairments. Linear ZF based chip level equalization has been one of the most popular equalizers for single user downlink CDMA [16]. Because of the noise enhancement in the ZF equalizers, we propose the application of the regularized zero forcing equalizer.
The time domain ZF estimation of **d** is given by [16]:

$$\mathbf{d}_{ZF} = (\mathbf{H}^H \mathbf{H})^{-1} \mathbf{H}^H \mathbf{r} \quad (27)$$

To encounter the problem of noise enhancement in ZF equalizers, a new regularization term is added into Eq. (27) to yields:

$$\mathbf{d}_{\mathbf{RZF}} = (\mathbf{H}^{\mathbf{H}}\mathbf{H} + \alpha\mathbf{I})^{-1}\mathbf{H}^{\mathbf{H}}\mathbf{r} = \mathbf{M}^{-1}\mathbf{H}^{\mathbf{H}}\mathbf{r} = \mathbf{G}\mathbf{r} \quad (28)$$

Where α is a regularization parameter .

The solution of Eq. (28) requires the inversion of the matrix **M** which has dimensions of (N×L)×(N×L). This inversion process is impractical in real time. Thus, a simplification is required for this inversion process.

The equalizer matrix **G** can then be easily calculated as follows:

$$\mathbf{G} = \boldsymbol{\Psi}\ \boldsymbol{\Lambda}_{M}^{-1}\boldsymbol{\Lambda}^{H}\boldsymbol{\Psi}^{-1} \quad (29)$$

where:

$$\boldsymbol{\Lambda}_{M}^{-1} = [\boldsymbol{\Lambda}^{H}\boldsymbol{\Lambda} + \alpha\mathbf{I}]^{-1} \quad (30)$$

The FDE-RZF algorithm can be summarized as follows:

1- Apply the FDE-RZF on the received signal as follows:

$$\mathbf{d}_{\mathbf{FDE-RZF}} = \boldsymbol{\Psi}\ (\boldsymbol{\Lambda}_{M}^{-1}\boldsymbol{\Lambda}^{H}\mathbf{R}_{T}) \quad (31)$$

3- Then, a better estimation of the symbol of interest can be obtained as follows:

$$\hat{\mathbf{b}}_{\mathbf{d}} = \mathbf{S}_{\mathbf{d}}^{T}\mathbf{C}^{H}\mathbf{d}_{\mathbf{FDE-RZF}} \quad (32)$$

4- Finally, discard the detected zero symbols at the end of each block, and then use the decision function.

A major advantage of this equalization method is its low computational complexity. The price to be paid is a reduction of the data rate caused by insertion of zero padding or cyclic prefix.

5.1 Complexity

The complexity of a P-point FFT is of the order of $P\log_2 P$. The FDE provides a complexity of $O(P \log_2 P)$ which shows a significant reduction as compared to that of the direct inversion of a matrix of dimensions P×P that has a complexity of the order of $O(P^3)$ [1]. The FDE has also less complexity than that of the RAKE receiver which has a complexity of $O(P^2)$ [1].

6 FDE-RZF WITH CLIPPER PIC

This section gives the proposed receiver which is used to improve the performance of the PIC for downlink CDMA. The proposed receiver uses the RAKE receiver with CPIC to estimate, regenerate, and cancel all the interfering users. Then the FDE-RZF equalizer is used to reduce the ISI effect and to provide better estimate of desired user's data. In this section, a specific data detection algorithm for downlink CDMA is derived which is based on FDE-RZF equalizer and CPIC. The proposed FDE-RZF-CPIC system model is depicted in Fig. (2).

The FDE-RZF-CPIC algorithm can be summarized as follows:

1- Estimate all interferences as follows:

$$\hat{\mathbf{I}}_{\text{int}} = \mathbf{U}^{T}\mathbf{C}^{H}\boldsymbol{\Psi}\ \boldsymbol{\Lambda}^{H}.\mathbf{R}_{T} \quad (33)$$

2- Discard the detected zero symbols at the end of each block to produce $\overset{L}{\mathbf{b}}_{\text{int}}$, then take the decision as follows:

$$\tilde{\mathbf{b}}_{\text{int}} = f_{dec}\{\overset{L}{\mathbf{b}}_{\text{int}}\} \quad (34)$$

where $f_{dec}(.)$ is a decision function that transforms the soft estimate into a unit clipper decision.

3- Add zeros for padding , then regenerate the MAI as follows:

$$\mathbf{r}_{MAI} = \mathbf{H}\ \mathbf{C}\mathbf{U}\ \tilde{\mathbf{b}}'_{\text{int}} \quad (35)$$

where $\tilde{\mathbf{b}}'_{\text{int}}$ is a zero padded version of $\tilde{\mathbf{b}}_{\mathbf{int}}$.

4-Use PIC to cancel the effects of interference on the received signal to get an interference free signal:

$$\mathbf{Z} = \mathbf{r} - \mathbf{r}_{\mathbf{MAI}} \quad (36)$$

5- Apply the FDE-RZF to the signal vector **Z** as follows:

$$\mathbf{d}_{\mathbf{FDE-CPIC}} = \boldsymbol{\Psi}\ (\boldsymbol{\Lambda}_{M}^{-1}.\boldsymbol{\Lambda}^{H}.\boldsymbol{\Psi}^{-1}(\mathbf{Z})) \quad (37)$$

6- Then, a better estimation of the symbols of interest can be obtained as follows:

$$\hat{\mathbf{b}}_{\mathbf{d}} = \mathbf{S}_{\mathbf{d}}^{T}\mathbf{C}^{H}\mathbf{d}_{\mathbf{FDE-CPIC}} \quad (38)$$

7- Finally, discard the detected zero symbols at the end of each block, and then use the decision function.

The performance of FDE-RZF-CPIC depends heavily on the channel estimate, not only in the detection step, but also in the interference regeneration step. It is more efficient when the system is heavily loaded.

7 CHANNEL ESTIMATION

In this section, we consider the channel estimation method which depends on the pilot signal. When the pilot sequence is transmitted, the received signal in Eq. (4) is expressed as:

$$\mathbf{r} = \mathbf{D}\mathbf{h} + \mathbf{n} \quad (39)$$

where the complex channel impulse response **h** is expressed as:

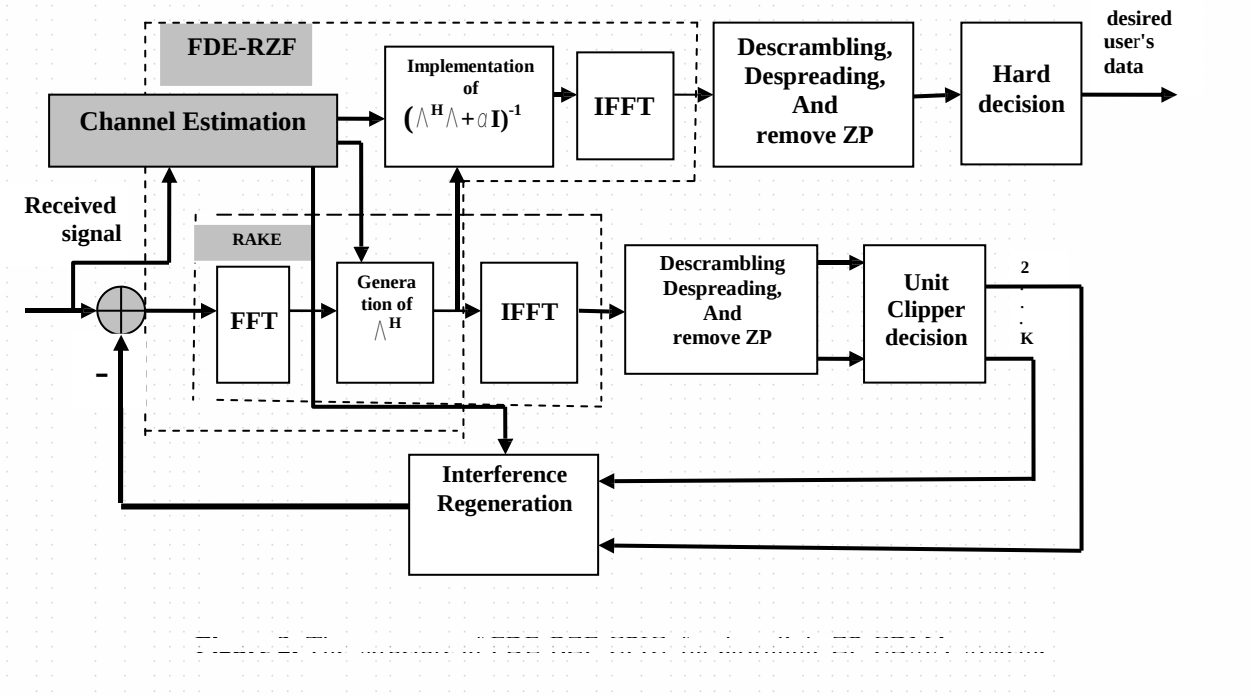

$$\mathbf{h} = [h_1, h_2, ..., h_W]^T \quad (40)$$

D is the circulant pilot sequence matrix.

The MMSE channel estimates are found by minimizing the following squared error quantity:

$$\hat{\mathbf{h}} = \arg\min_{\mathbf{h}} \|\mathbf{r} - \mathbf{D}\mathbf{h}\|^2 \quad (41)$$

Assuming white gaussian noise, the ZF solution is given by:

$$\hat{\mathbf{h}}_{ZF} = (\mathbf{D}^H\mathbf{D})^{-1}\mathbf{D}^H\mathbf{r} \quad (42)$$

However, using zero forcing channel estimation, the channel estimation accuracy significantly degrades due to the noise enhancement.

8 SIMULATION RESULTS

Several simulation experiments are carried out to test the performance of the proposed FDE-RZF-CPIC algorithm and compare it to other algorithms. The simulation environment is based on the downlink synchronous ZP-CDMA system, in which each user transmits BPSK symbols. These symbols are spread. After spreading, the resulting sum signal is scrambled using a complex scrambling sequence. The propagation channel is taken to be chip-spaced with delay spread of $3T_c$. For all simulations, we take N=16, and the block size is N_F=256 chips with 16 zeros (N_{ZP}=16) at the end of each block as shown in Fig. (1). All users are assigned the same power.

Figure 3 compares the performance of the FDE-RZF and that of the TDE and the RAKE receiver for 8 users . It is clear that the equalization in the time domain is identical to that in the frequency domain. The only difference is in the method of implementation. Both equalizers have better performance than that of the RAKE receiver only.

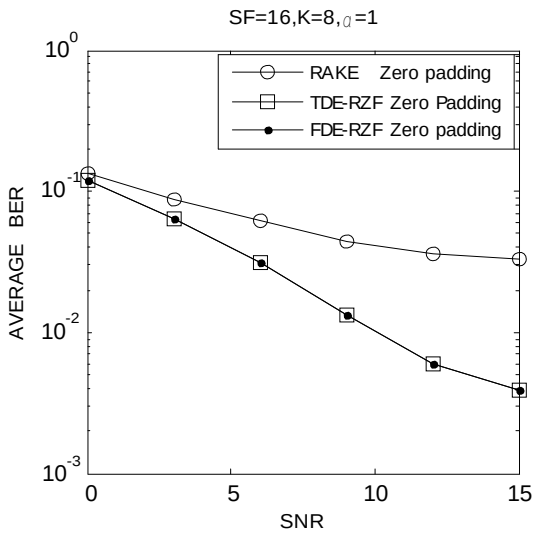

Figure 3: Performance of FDE-RZF, TDE-RZF and RAKE receiver Vs the SNR .

The performance of the RAKE receiver with PIC and different decision functions is studied. Figures 4, and 5 illustrate the average BER versus the threshold of the null zone decision function (c_n) at different SNR values and different number of users.

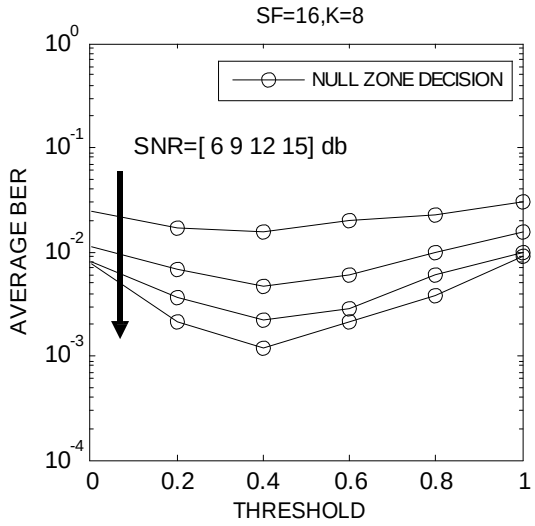

Figure 4: Performance of the RAKE receiver with PIC Vs null zone decision threshold (c_n) at different SNRs .

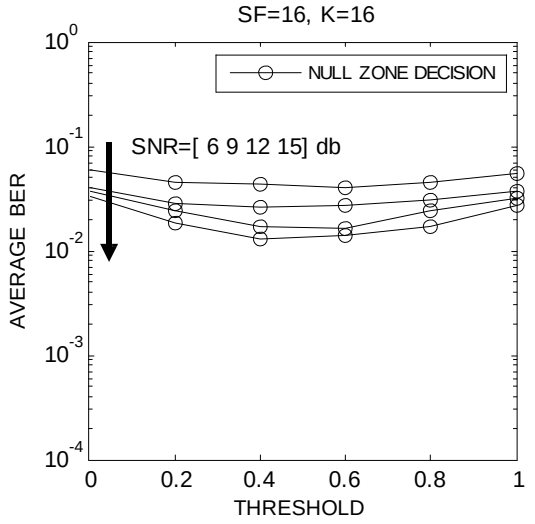

Figure 5: Performance of RAKE with PIC Vs null zone decision threshold (c_n) at different SNR .

The optimal performance is obtained when c_n=0.4. Figures 4, and 5 show that c_n is non-sensitive to SNR-changes and to system-load changes.

The effect of the tentative decision function on the performance of PIC for K=8 (half loaded), and K=16 (Full loaded) are studied and shown in Figs. 6, and 7. As the number of users increases, the performance deteriorates. The performance of a single-user RAKE receiver is very poor, even for high SNR values. Parallel interference cancellation improves the performance significantly. Better performance can be obtained with the clipper decision function. Linear decision performance is worse than that of the single user RAKE receiver for the heavily loaded case (K=16). This is justified by the fact that PIC with linear decision is limited by noise enhancement.

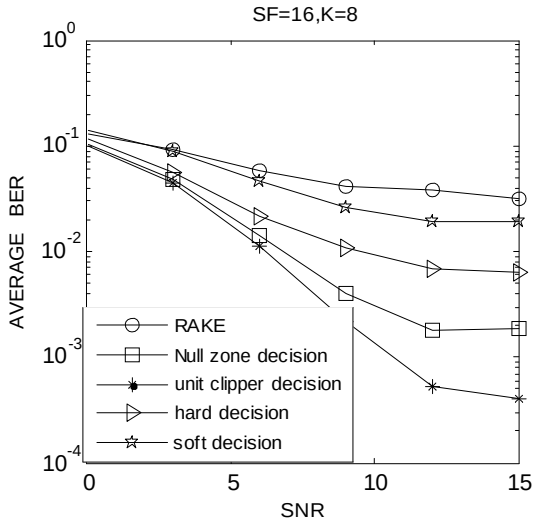

Figure 6: Performance of the RAKE receiver with PIC at different decision functions Vs the SNR for the half loaded case. c_n=0.4.

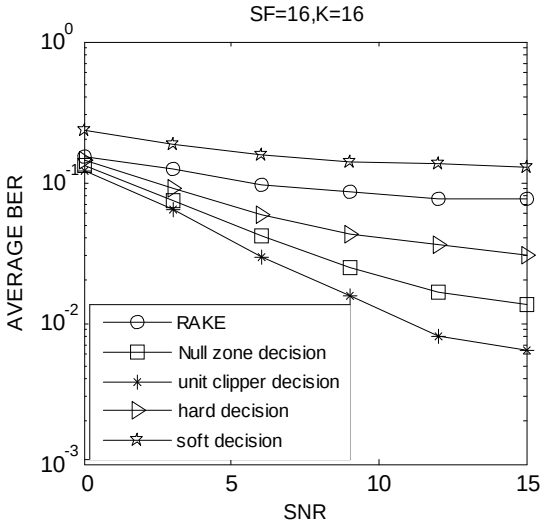

Figure 7: Performance of the RAKE receiver with PIC at different decision threshold functions Vs the SNR for a full loaded case. c_n=0.4.

The performance of the proposed FDE-RZF-CPIC is compared to that of the RAKE receiver, FDE-RZF equalizer, the RAKE receiver with hard decision PIC, and the RAKE receiver with unit clipper decision PIC.

The effect of the regularization parameter on the performance of FDE-RZF-CPIC is examined in two experiments and shown in Figs. 8 and 9. The optimal

value of the regularization parameter α is equal to 1. This value is neither sensitive to SNR-changes nor to system-load changes.

The effect of the choice of the tentative decision function on the performance of the proposed receiver is studied (Fig. 10). The performance with clipper decision outperforms the performance with all other decision functions .

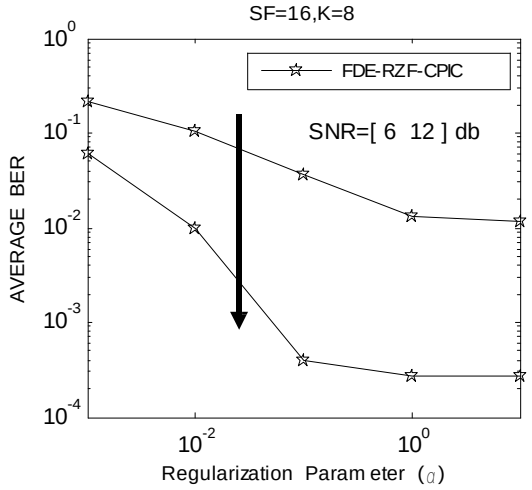

Figure 8: Performance of FDE-RZF-CPIC scheme Vs regularization parameter (α) at different SNR for a half loaded system. .

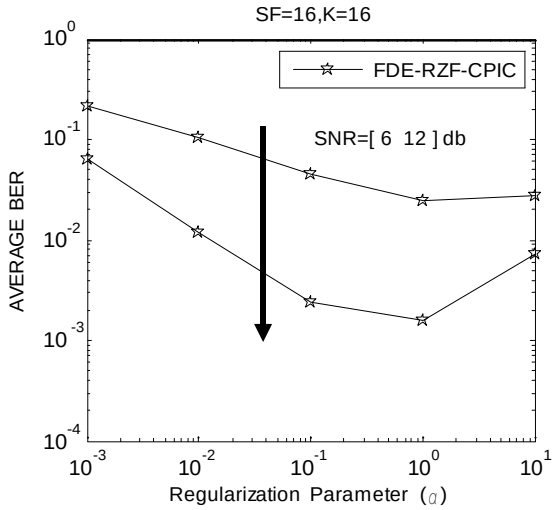

Figure 9: Performance of FDE-RZF-CPIC scheme Vs regularization parameter (α), at different SNR for a full loaded system..

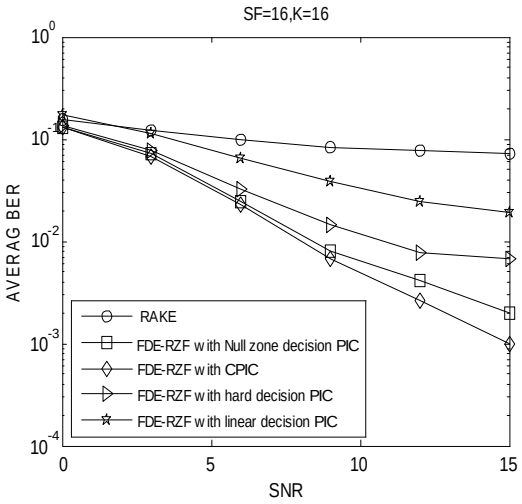

Figure 10: Performance of the proposed receiver at different decision Functions Vs the SNR.

Figures 11, and 12 show the performance of five reception schemes as a function of SNR of each user for 8 and 16 users, respectively. From Figs. 11, and 12, it can be observed that there is a clear improvement achieved by FDE-RZF–CPIC scheme over other reception schemes. In Fig. 12, BER performances of all receivers are worse than the performances in Fig. 11 because of the increment in the number of users. The FDE-RZF-CPIC scheme improves the performance significantly, without saturation of the performance for high SNRs like the RAKE receiver. For the heavily loaded case (Fig. 12), the performance of FDE-RZF equalizer is greater than that of the RAKE with PIC scheme. This can be explained by the fact that at heavily loads, the RAKE receiver sees too much interference, which makes its decisions about interfering users unreliable.

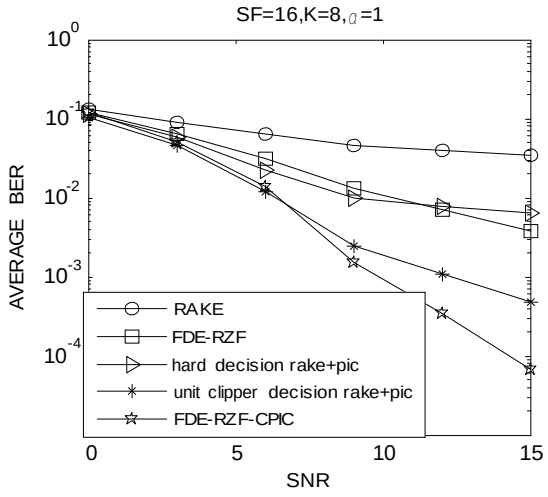

Figure 11: Performance of different reception schemes Vs the SNR for a half loaded system.

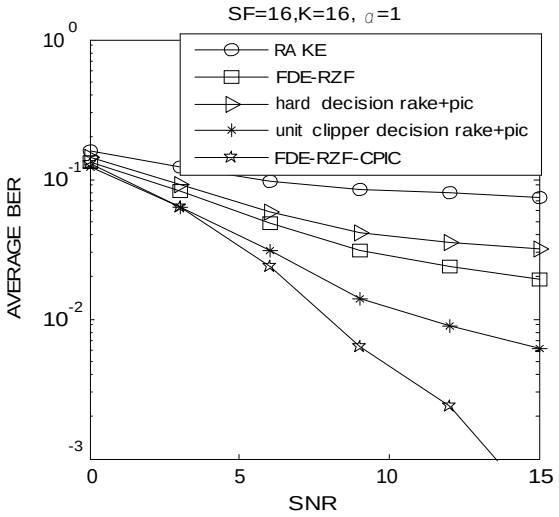

Figure 12: Performance of different reception schemes Vs the SNR for a full loaded system.

The effect of user loading on the performance of the FDE-RZF-CPIC scheme is studied and presented in Fig. 13. The BER of all receivers degrade with increasing the number users. In this case, the BER performance of FDE-RZF-CPIC scheme degrades a little bit with increasing the number of users, but it is still better than the other schemes. This observation may be due to the MAI. The MAI when the number of users is large should be greater than the case when the number of users is low. Even after interference cancellation, some residual MAI still exists. Therefore, the performance loss may be attributed to the residual MAI.

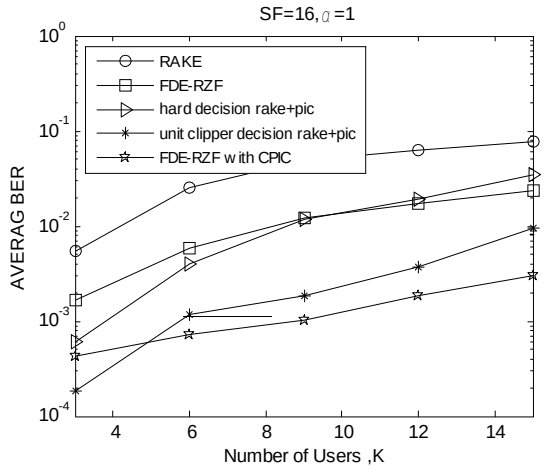

Figure 13: Performance of different reception schemes Vs the number of active users. and SNR =12 dB.

Figure 14 depicts the average BER performance as a function of the number of cancelled users, at a fixed SNR per user of SNR=12 dB. This graph shows that the performance of the FDE-RZF-CPIC scheme improves when the number of cancelled users increases.

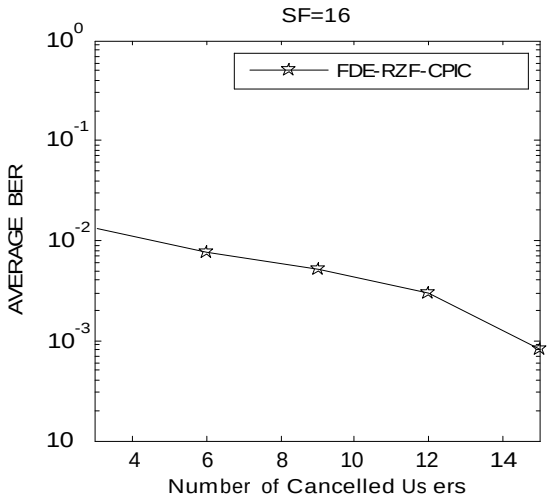

Figure 14: Performance of FDE-RZF-CPIC scheme Vs number of canceled users. =1, and SNR =12 dB.

The effect of channel estimation accuracy on the performance of the FDE-RZF-CPIC scheme for K=8 are studied and shown in Figs. 15, and 16. The performance of FDE-RZF-CPIC scheme with ZF channel estimation shows a loss of 1 dB at BER of 10^{-2} when compared with the case of perfect channel knowledge. Because the noise enhancement in the ZF channel estimation. LMMSE channel estimation gives better performance.

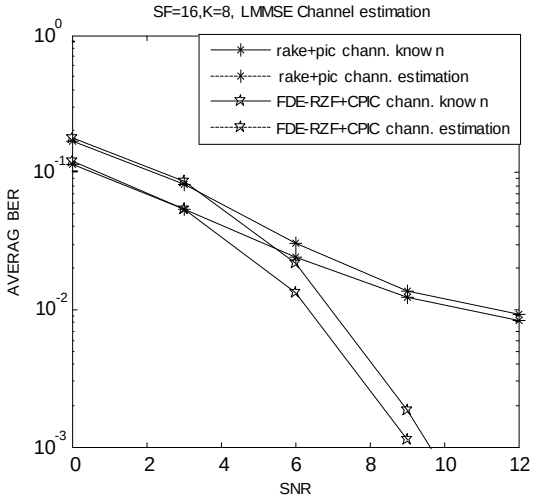

Figure 15: Performance of Interference Cancellation Vs the SNR for exact and LMMSE channel estimate.

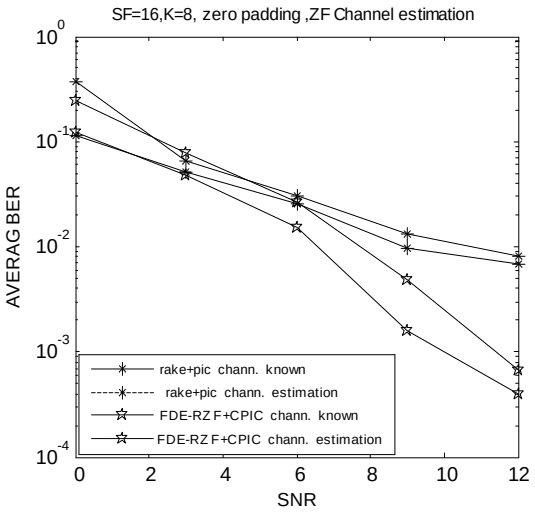

Figure 16: Performance of Interference Cancellation Vs the SNR for exact and ZF channel estimate.

9 CONCLUSION

The paper presents an efficient FDE-RZF-CPIC receiver for downlink CDMA. This receiver is implemented using frequency domain approximations rather than the time domain implementation to reduce complexity. The comparison studies show that the proposed receiver outperforms several traditional receivers for different loading cases. The sensitivity of the proposed receiver is also studied for different decision functions and different channel estimation methods. The obtained results indicate that the proposed receiver performance is robust for the different channel estimation methods.

APPENDEX 1 Toeplitz to circulant approximation

Let $\mathbf{Q}$ be an *SXS* Toeplitz matrix of the following form:

$$\mathbf{Q} = \begin{bmatrix} q(0) & \cdots & q(-l) & \mathbf{0} \\ \vdots & \ddots & & \ddots \\ q(k) & & \ddots & q(-l) \\ & \ddots & & \vdots \\ \mathbf{0} & q(k) & \cdots & q(0) \end{bmatrix} \quad \text{(A.1)}$$

It can be approximated by an *SXS* circulant matrix $\mathbf{Q^c}$ defined as [17,18]:

$$\mathbf{Q^c} = \begin{bmatrix} q(0) & \cdots & \cdots & q(-l) & 0 & \cdots & q(k) & \cdots & q(1) \\ \vdots & \ddots & & & \ddots & \ddots & \cdots & \ddots & \\ \vdots & & \ddots & & & \ddots & \ddots & \cdots & q(k) \\ q(k) & & & \ddots & & & \ddots & \ddots & \cdots \\ 0 & \ddots & & & \ddots & & & \ddots & 0 \\ \vdots & \ddots & \ddots & & & \ddots & & & q(-l) \\ q(-l) & \vdots & \ddots & \ddots & & & \ddots & & \vdots \\ \vdots & \ddots & \vdots & \ddots & \ddots & & & \ddots & \vdots \\ q(-1) & \cdots & q(-l) & \vdots & 0 & q(k) & \cdots & \cdots & q(0) \end{bmatrix} \quad \text{(A.2)}$$

where each raw is a circular shift of the raw above and the first raw is a circular shift of the last raw. The primary difference between the matrices $\mathbf{Q}$ and $\mathbf{Q^c}$ is that they differ only by elements added in the upper right and lower left parts to produce the cyclic structure in the raws. If the matrix size S is large and the number of non zero elements on the main diagonals compared to the number of zero elements is small (i.e the matrix is sparse), the number of elements added to the upper right and lower left parts does not affect the matrix, because they are small in proportion to the main diagonal elements. It can be shown from the eigen value distribution of both matrices that $\mathbf{Q}$ and $\mathbf{Q^c}$ are asymptotically equivalent.

It is known that an *SXS* circulant matrix $\mathbf{Q^c}$ is diagonalized by [1]:

$$\mathbf{\Lambda} = \Psi^{-1}\mathbf{Q^c}\Psi \quad \text{(A.3)}$$

where $\mathbf{\Lambda}$ is an *SXS* diagonal matrix whose elements $\lambda(s,s)$ are the eigenvalues of $\mathbf{Q^c}$ and where Ψ is an *SXS* unitary matrix of eigen vectors of $\mathbf{Q^c}$. Thus we have:

$$\Psi\Psi^{*\mathbf{t}} = \Psi^{*\mathbf{t}}\Psi = \mathbf{I} \quad \text{(A.4)}$$

The elements $\psi(s_1, s_2)$ of Ψ are given by [17,18]:

$$\psi(s_1, s_2) = \exp\left[\frac{j2\pi s_1 s_2}{S}\right] \quad \text{(A.5)}$$

for $s_1, s_2 = 0,1,.....,S-1$ and $j^2 = -1$

The eigen values $\lambda(s,s)$ can be called $\lambda(s)$. For these eigen values, the following relation holds [17,18]:

$$\lambda(s) = q(0) + \sum_{m=1}^{k} q(m)\exp\left[\frac{-j2\pi ms}{S}\right] + \sum_{m=-l}^{-1} q(m)\exp\left[\frac{-j2\pi ms}{S}\right] \quad \text{(A.6)}$$

$s = 0,1,.....,S-1$

Because of the cyclic nature of $\mathbf{Q^c}$, we define:

$$q(S-m) = q(-m) \quad \text{(A.7)}$$

and thus Eq.(A.6) can be written in the form [17,18]:

$$\lambda(s) = \sum_{m=0}^{S-1} q(m)\exp\left[\frac{-j2\pi ms}{S}\right] \quad \text{(A.8)}$$

for $s = 0,1,.....,S-1$

Thus the circulant matrix can be simply diagonalized by computing the DFT of the cyclic sequence $q(0), q(1),....., q(S-1)$.

10 REFERENCES

[1] I. Martoyo, T. Wesis, F. Capar, and F.Jondral, "Low complexity cdma downlink receiver based on frequency domain equalization," *in Proc. IEEE Vech. Tech.. Conf.*, pp. 987-991, Oct. 2003.

[2] J. Pan, P. De, and A Zeira, "Low complexity Data Detection Using Fast Fourier Transform Decomposition of Channel Correlation Matrix, " *IEEE Global Telecom. Conference*, vol. 2 , pp. 1322-1326, Nov. 2001.

[3] D. Falconer, S. L. Ariyavisitakul, A. Benyamin-Seeyar, and B. Edison, "Frequency domain equalization for single-carrier broadband wireless systems," *IEEE Mag. Commun.*, Vol. 40, no. 4, pp. 58-66, Apr. 2002.

[4] F. petre, G. Lues, L. Deneire, and M. Moonen, "Downlink frequency domain chip equalization for single-carrier block transmission ds-cdma with known symbol padding," *in Proc. GLOBCOM*, pp. 453- 457, Nov. 2002 .

[5] K.L. Baum, T.A. Thomas, F.W Vook, and V. Nangia, "Cyclic-prefix CDMA: an Improved Transmission Method for Broadband DS-CDMA Cellular Systems," *IEEE Wireless Comm. And Networking Conference*, vol. 1, pp.17-21, Mar. 2002.

[6] B. Mouhouche, K. Abed-Meraim, N. Ibrahim, and P. Loubaton, "Combined MMSE equalization and blind parallel interference cancellation for downlink multirate CDMA communications," *IEEE 5th Workshop on Signal Processing Advances in Wireless Communications*, pp. 492–496, 11-14 July 2004.

[7] B. Mouhouche, K. Abed-Meraim, and S. Burykh, "Spreading code detection and blind interference cancellation for DS/CDMA downlink," *IEEEISS STA '04*, Sydney, Australia, pp. 774-778, 2004.

[8] Z. Gao, Q. Wu, and J. Wang, "Combination of LMMSE equalization and multi-path interferen-ce cancellation in WCDMA receivers" *IEEE ICMMT 4th International Conference*, pp. 838–841, 18-21 Aug. 2004.

[9] M.F. Madkour, S. C. Gupta, and Y. .E. Wang, "Successive Interference Cancellation Algori-thms for Downlink W-CDMA Communications, " *IEEE Trans. Wireless Comm.*, vol. 1, N. 1 , January 2002.

[10] L. B. Nelson, and H. V. poor, "Iterative multiuser receivers for CDMA channels: An EM- based approach," *IEEE Trans. Commun.*, Vol. 44, pp. 1700-1710, Dec. 1996.

[11] A. L. C. Hui, and K. B. Letaief, "Multiuser asynchronous DS/CDMA detectors in multipath fading links, " *IEEE Trans. Commun*., vol. 46, pp. 384–391, Mar.1998.

[12] W.Zha, S., and D. Blostein , "Soft-decision multistage multiuser interference cancellation, " *IEEE Trans. Techn*., Vol. 52, No. 2, pp. 380-389, 2003.

[13] A. Klein, G. K. Kaleh, and P. W. Baier, "Zero Forcing and Minimum Mean-Square-Error Equalization for Multi-User Detection in Code Division Multiple-Access Channels," *IEEE Trans. Vehic. Tech.*, vol. 45, no. 2, pp. 276-87 May 1996.

[14] S. Werner, and J. Lilleberg, "Downlink channel decorrelation in CDMA systems with long codes," *IEEE 49th Vehicular Technology Conference*, vol. 2, pp. 1614–1617, 16-20, 1999.

[15] M. Varanasi, and B. Aazhang, "Multistage detection in Asynchronous Code-Division Multiple Access Communications," *IEEE Trans. Commun.* , 38(4), pp. 509-519, 1990.

[16] A. Klein, "Data detection algorithms specially designed for the downlink of CDMA mobile radio systems," *IEEE 47th Vehicular Technology Conference*, vol. 1, pp. 203–207, 4-7 May 1997.

[17] H.C. Anderws and B.R. Hunt, Digital Image Restoration. Englewood Cliffs, NJ: Prentice-Hall, 1977.

[18] Jan Biemond , Jelle Rieske and Jan J. Gerbrands, "A Fast Kalman Filter For Images Degraded By Both Blur And Noise," IEEE Trans. Acoustics, Speech and Signal Processing, Vol. ASSP-31, No.5, pp.1248-1256, Oct. 1983.